DETERIORATED SAMPLES USING MILLI X-RAY

FLUORESCENCE -X-RAY SPECTRUM IMAGING

By

HARISHMA DONTHINENI

Bachelor of Technology in Civil Engineering

Gayatri Vidya Parishad College of Engineering

Visakhapatnam, Andhra Pradesh - India

2013

Submitted to the Faculty of the
Graduate College of the
Oklahoma State University
in partial fulfillment of
the requirements for
the Degree of
MASTER OF SCIENCE
July, 2015

CHEMICAL PROFILING OF SULFATE

DETERIORATED SAMPLES USING MILLI X-RAY

FLUORESCENCE -X-RAY SPECTRUM IMAGING

Thesis Approved:

Julie Ann Hartell, PhD

Thesis Adviser

Tyler. M. Ley, PhD, P.E

Committee Member

Stephen. A. Cross, PhD., P.E.

Committee Member

ACKNOWLEDGEMENTS

I would like to express my heartfelt gratitude to Dr. Julie Ann Hartell (advisor) for her constant moral support and amazing motivation all through my master's degree. She is a great adviser who encouraged me to work on different research projects, inspired us to manage things accordingly and always supporting us through all of our mistakes.

I would like to thank my committee member Dr. Tyler Ley for his timely guidance and support. My sincere thanks to Mr. Mehdi Khanzadeh Moradlo for training me on various equipment and for guiding me in my research from the start till the end.

I dedicate this thesis to my parents Mr. Nageswara Rao Donthineni and Mrs. Bhagya Lakshmi Donthineni who have always supported me in and out, all through my 24 years to make my dreams come true.

I would like to extend my thanks to my friends Mr. Wassay Gulrez, Ms. Meher Mandavilli and Mr. Ignatius Vasant for helping me during the research hours and making it an easy task to work in civil engineering laboratory. I would like to thank each and every friend in OSU who energized me to finish my research and reach my landmark.

Name: HARISHMA DONTHINENI

Date of Degree: JULY, 2015

Title of Study: CHEMICAL PROFILING OF SULFATE DETERIORATED SAMPLES USING MILLI X-RAY FLUORESCENCE -X-RAY SPECTRUM IMAGING

Major Field: CIVIL ENGINEERING

Abstract:

External sulfate attack damages the structures exposed to various environmental conditions. In order to understand the damage of concrete structures with the ingress of sulfate ions, it is essential to recognize the path of sulfates into the concrete at different exposure conditions. Exposure conditions are mostly based on the real time conditions of the structures; hence partially saturated conditions, wet-dry cycles, saturated conditions are used to get a close picture of field conditions. Concrete cylinders, cast from a 0.48 w/c ratio were completely and partially exposed to 5% sodium sulfate solution for a period of two years. After two years, there was good evidence of physical degradation and this occurred due to different chemical interactions for the period of time. Milli-x-ray fluorescence technique is used to map the sulfur profile of the sulfate deteriorated samples. This gave a clear picture of the concentration levels in the concrete derived from an external source of sulfates. It also provided insight on how the sulfur ions travelled within the concrete matrix with respect to the different transport mechanisms analyzed. It was found that the presence of an evaporation plane, creating a wicking transport mechanism, did contribute to drawing a larger amount of sulfates deeper into the matrix.

TABLE OF CONTENTS

LIST OF TABLES

LIST OF FIGURES

CHAPTER 1

INTRODUCTION

When expansion and cracking occur in hardened cement paste due to the penetration of sulfate ions, it is termed as sulfate attack. It results in overall loss of strength of the material. Traditional test methods to evaluate sulfate degraded concrete include monitoring the change of length and mass of specimens, strength testing, visual assessment (Bonakdar et al. 2010). Recently, advanced analytical techniques such as scanning electron microscopy- energy dispersive spectroscopy (SEM-EDS), petrographic analysis are used to identify the presence of sulfate in the concrete matrix and qualify the extent of damage. Analytical tools such as X-ray diffraction and X-ray fluorescence analysis, which provide structural and elemental information respectively for a variety of inorganic material, have also been used to identify the presence of sulfate compounds in concrete.

There are many types of analytical methods using X-ray focused beams to analyze specimens but, for the purpose of this study, a technique named milli X-ray Fluorescence X-ray Spectrum imaging (mXRF-XSI) capable of providing compositional maps over large sample area will be used to investigate concrete samples exposed to an external source of sulfates. The method can provide a quantitative and qualitative picture of various precision using point, line or area scanning techniques.

Since external sulfate attack (ESA) can occur due to the exposure of sulfates from ground water or other environmental conditions, this study replicates various transportation mechanism depicting field conditions: diffusion, advection, sorption, evaporation to name a few. Three types of exposure conditions are investigated, namely complete immersion, partial immersion and cyclic immersion which depict real mechanisms encountered. For these, the effects of the combination of transport mechanisms are not well understood. For example, as per Boyd and Mindness 2004, the bulk wicking action created by partial immersion caused salt recrystallization at the evaporative surface; however, Himes 2005 claimed that capillary suction is responsible for sulfates traveling upwards along the surface only of the partially immersed cylinder. Visually, both principles result in voids and cracks filled with salts and by-products formed due to ESA. However, the extent of overall damage may vary according to the path the sulfates traveled.

This research attempts to provide an image of that path using mXRF elemental imaging of sulfate ions for the different exposure conditions afore mentioned. After detecting the presence of sulfate ions at different depths, it was possible to recognize certain differences between three the exposure conditions and make evident conclusions regarding sulfate transport.

CHAPTER 2

REVIEW OF LITERATURE

In this chapter, a major portion, section 2.1, concentrates on reviewing the principles of external sulfate attack on concrete and their mechanisms along with past investigation conducted on the matter. When we say mechanisms, it involves both physical and chemical changes along the transport path of sulfate inside the concrete matrix. These transport mechanisms lead to sulfate ingress and deterioration of concrete.

It was found that many different analytical methods have been used for investigating sulfate ingress. Recently, for the quantification of sulfur and its by-products, advancements have been made in the field of microscopy to get more accurate data. These methods are discussed in detail in section 2.2.

2.1. External Sulfate Attack Mechanisms

As in, the external sulfate attack is described as the extensive cracking or expansion losses at the bond between cement paste and aggregate due to the penetration of sulfates containing water into the concrete matrix. This leads to formation of ettringite and gypsum in later stages. (Cohen et al. 2003)

"Sulfate attack can be defined as set of mineralogical changes with physical effects and is generally attributed to the formation of ettringite from the interaction between sulfate and alumina- bearing phases in the cement".

Sulfate attack is distinguished into two types – internal and external. The sulfate ions obtained from aggregates or the cement paste are considered to be internal and those from the surroundings to be external. (Peukert et al. 1999).

External Sulfate attack (ESA) is a chemical breakdown mechanism where the components of cement paste come across sulfate ions from external source. In general the sulfates attack concrete through ground water, sea water, sewage water etc. The microscopic appearance of concrete suffering from ESA have some peculiar qualities like surface parallel cracks, presence of gypsum and ettringite, depletion of calcium hydroxide and decalcification of C-S-H. (Jakobsen, 2006)

The microstructural changes in the concrete due to the attack of sodium sulfate and magnesium sulfates are well explained by Santanam et.al. 2003. When sodium sulfate ion comes in contact with mortar, three types of discrete zones are formed: a cracked and highly deteriorated surface zone (Zone 1) and this is followed by a zone of deposition of sulfate attack products (Zone 2). In zone 2, gypsum around aggregates and in pores can be found principally along with ettringite within the paste. This zone is followed by the interior chemically unaltered zone (Zone 3) which may be cracked. When magnesium sulfate solution comes in contact with concrete, a brucite surface layer is formed where the gypsum and ettringite gets attached at the bottom of barrier created by brucite and at the high concentrated regions the C-S-H converts into M-S-H as the brucite layer breaks.

Step 1 of Figure 2.1, shows the initial condition of mortar introduced to sodium sulfate solution where the pH is low. After a period of time, step 2, it continues to increase and forms gypsum and ettringite at the surface which causes expansion stresses (while in the Step 3). Then, there is resistance from mortar causing cracks to occur and over period of time, as in Step 4, voids and cracks are filled with gypsum because they provide best sites for nucleation. In step 5 new cracks

form inside the concrete and, in step 6, the three zones are formed where the complete disintegration takes place. (Santhanam et al., 2002).

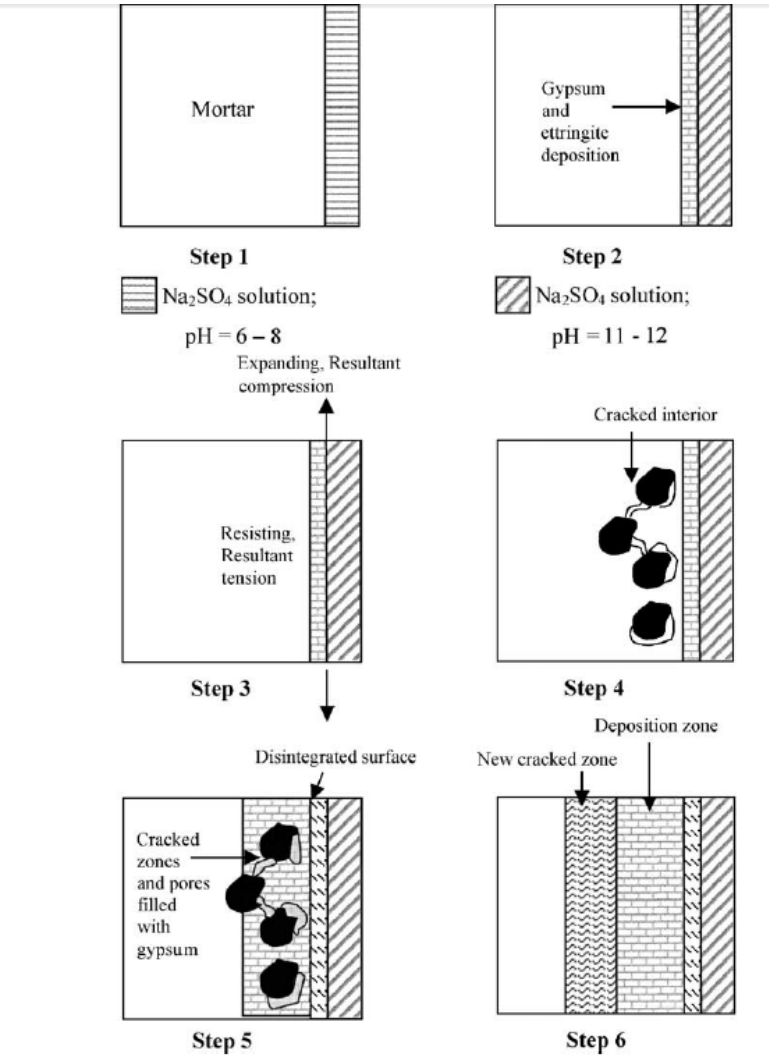

Figure 2.1. Mechanism of sulfate attack

(Santhanam et al., 2002)

2.1.1 Chemical Reactions Involved In External Sulfate Attack

The three main crystalline products formed due to the reaction between cement hydrates and sulfate ions are:

1. ettringite (Ca6(Al,Fe)2(SO4)3(OH)12.26H2O; hexagonal) with expansive nature;
2. gypsum (CaSO4.2H2O; monoclinic);
3. thaumasite (3CaO.SiO2.SO4.CO3.15H2O; hexagonal

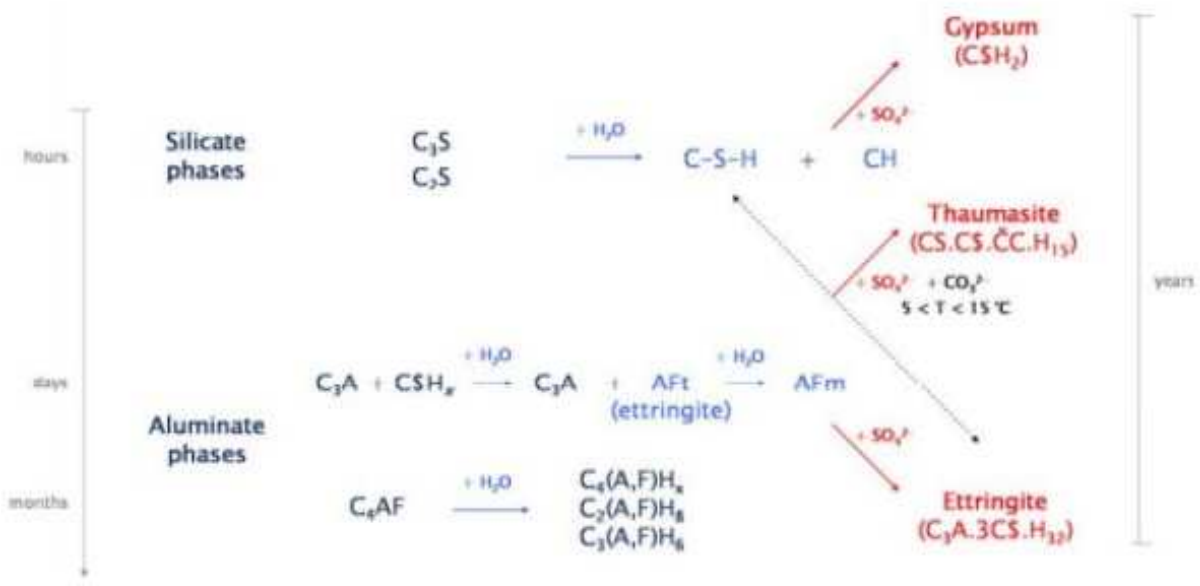

Figure 2.2. Reaction products of ESA

(Matschei 2007)

As seen in Figure 2.2, ettringite is formed from C_3A and its hydration products in the cement paste or from the fly ash compound of aluminate-bearing glass. CH reacts with sulfate ion to give gypsum. In order to form thaumasite to form, CSH needs to react with sulfate ion in the presence of carbonate and at low temperatures (Matschei 2007).

2.1.2 Damage Mechanisms

Ettringite formation leads to expansion which causes cracking and spalling of concrete. The formation of these very small crystals within the capillary space are the reason for the observable distress in the paste compared to crystal formation in larger cavities. Also, ettringite and gypsum

formation together lead to the decalcification of C-S-H phase resulting in paste softening. In turn, thaumasite formation, a product formed by combination of carbonate (sulfate source) and silicon (from C-S-H) is the cause for decohesion (Gollop et al., 1995).

2.1.3 Sulfate Transport Mechanisms

Sulfate attack by external sources is based on transport mechanism leading to changes in mineralogy between the surface and in depth regions which can be related directly to the uptake of sulfate along with leaching. (Bonen et al., 1992)

The possible transport mechanisms are diffusion, absorption, permeation which leads to the deterioration of the concrete by reaction of the external ions with concrete constituents in the pore structure. These mechanisms due to the combination differential pressure, temperature, concentration and humidity of solutions. (Basheer et al., 2001)

2.1.3.1 Permeability

Under the differential pressure the ease with which a fluid will flow into the concrete is termed as permeability. Permeability cells are used to measure the flow of the fluid under pressure, by applying pressure at one side and measuring the rate of flow on the other side of the sample (Basheer L et al., 2001).

2.1.3.2 Diffusion

In the fully saturated solution, the ion exchange takes place and the pore solution consists of alkalis combined with OH- and Ca(OH)2, making the solution pH equals to 12-13. The outer environment acts as an acid and leaches away all the cations and making it poor in Ca ions. Thus the ettringate replace monosulfoaluminate in concrete, with portlandite dissolution, C-S-H decalcification.

2.1.3.3 Absorption

The wetting and drying cycles causes weathering and the concrete acts like a porous membrane by absorption and evaporation and by leaving the resultant precipitated salts as end products. "Sodium salt exists as an anhydrate called thenardite, Na_2SO_4, or as a decahydrate called mirabilite, $Na_2SO_4.10H_2O$. At room temperature and at relative humidity RH < 75 %, mirabilite decomposes to thenardite. In presence of wetting and drying cycles this implies repeated thenardite recrystallization. This temperature and humidity dependent process causes repeated increase in volume leading to fatigue of the cement paste causing a cohesion loss."(Gollop et al. 1995) Capillary sorption rate depends on the degree of saturation of the concrete porous structure and it is controlled by temperature, evaporation rate, wet-dry cylces (Gollop et al. 1995).

2.1.3.4 Wicking action

The partially submerged concrete comes across the capillary rise and followed by evaporation. Due to the diffusion of the salts crystal efflorescence occurs in the supersaturated conditions. The moisture gradient helps the sulfate solution to fill up the unsaturated regions of concrete and the nucleation and crystalline growth leads to the formation of cracks due to expansive forces.

There is a lot of difference between saturated concrete and partially submerged concrete exposed to wet-dry cyles, where the saturated condition are not applied in the real field. Since, here only diffusion takes place with the reactions between calcium hydrates and sulfates, the reaction speed is slow (Taylor H. F.W et al., 1997).

2.2 Analytical Methods for Investigating Sulfate Ingress

2.2.1 Scanning Electron Microscopy

Scanning Electron Microscopy is used to identify the profile of ions in microstructure of the concrete using elemental maps. This is used to obtain composition, phase abundance and distribution data for quantitative analysis. Electron beam interaction with the samples gives the signals, and they can be used to measure chemical composition, phase distribution. Secondary electron imaging is used to determine the surface topography. Backscattered electron imaging is technique uses high energy beam electrons to get a contrast image of different phase compositions and in this case anhydrous cement turn out brightest among all cement compounds (Stutzman et al. 2001).

2.2.2 Optical spectrum analyzer

Optical fiber sensors detects the shift in refractive index of the concrete due to the presence of sulfates or chlorides with the help of ultra violet rays or laser. Optical spectrum analyzer is used to obtain the refractive index, with the help of transmission spectra (Torres, 2014).

Laser induced breakdown spectroscopy (LIBS) is a spectroscopic method providing information about the elemental compositions of materials. The sulfur spectral line at 921.3 nm is suitable for quantitative sulfur detection in building materials (Weritz et al., 2005). The measurements were accomplished in the wavelength range from 885 nm to 945 nm. The spatial resolution closes a gap between macroscopic chemical analysis and microscopic methods like XRF or SEM. Thus, LIBS has a great potential for damage assessment, quality assurance and service life and durability considerations of constructions exposed to sulfates. This method has good tolerance against environmental conditions such as dust and vibrations, and it is also possible to measure without sample preparation which makes it suitable for onsite application.

2.2.3 Micro-X-ray fluorescence and X-ray diffraction techniques

Micro-XRF mappings is based on the ability of X-rays to excite elements to emit a characteristic fluorescence radiation using the semiconductor detector. This is more advantageous than SEM because of the ease of the sample preparation. X-ray diffraction analysis is based on the diffraction of the crystalline phases. At a given wavelength, each crystalline phase has its own diffraction pattern (Taylor et al.1997)

X-ray fluorescence analysis is a method in which a beam of monochromatic x-rays on the incident range emits radiations from the sample. These are the characteristic of phase and chemical composition of the ions. This process is a non-destructive and efficiently used for quantification of phase present in bulk crystal structure. This analysis is more suitable for wide area scans on the samples with larger aggregate grains (Stroh et al., 2014).

2.2.4 Milli X-ray Fluorescence X-ray Spectrum Imaging

Fluorescent x-rays are emitted as the sample is excited with the passage of x-rays and the intensities are transformed into pixels. Every element will have its own characteristic signal to produce different concentrations. This can differentiate the cement paste and aggregates elemental composition. Bryan, 2013 used this techniques to find out the silane layer in the concrete structure. The m-XRF analysis is used to create the elemental maps and find out the area bands consisting of high amounts of sulfur to investigate the presence of silane layer. This analysis is further crosschecked by dipping the concrete in chlorine based colored dye (Figure 2.3); which is rescanned to recognize the silane band which do not absorb the color and results in a contrast picture to the before process (Bryan, 2013).

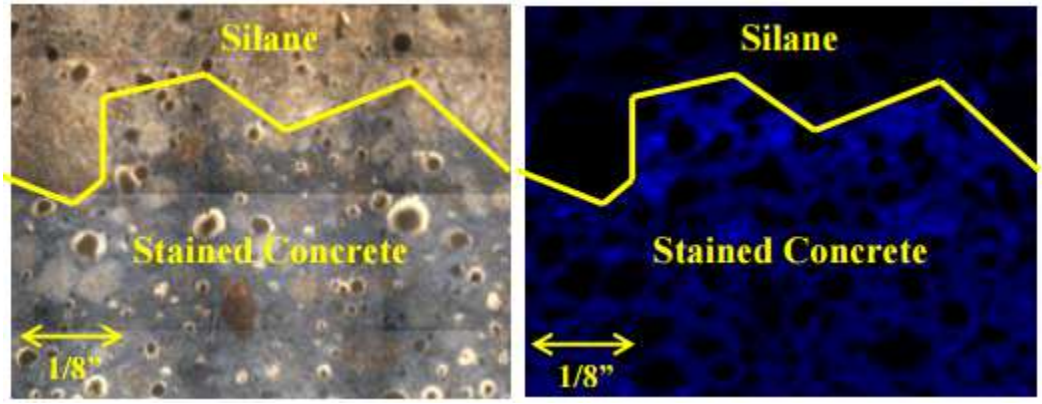

Figure 2.3 μ-XRF image of elemental mapping and optical image of colored dye

(Bryan, 2013)

CHAPTER 3

EXPERIMENTAL METHODOLOGY

In this study, sulfate-degraded concrete samples are examined to investigate sulfate transport mechanisms for different exposure conditions. To accomplish such, mXRF was used to produce a quantitative elemental map of sulfur in order to compare various transport mechanisms simulated in a laboratory environment and investigate the extent of sulfate ingress in the concrete samples. The present chapter elaborates on the fabrication of the samples, their exposure conductions and experimental work performed.

3.1 Specimen Fabrication and Conditioning

Table 3.1: Mixture Design

Material	Description	Quantity(kg)	
		1.00 m3	0.055 m3
Water	Potable, city of Montreal	217.45	11.96
Cement	Type GU	448.18	24.65
Coarse aggregate	5-14 mm, Granite rock, St-Hippolyte quarry (dry)	848.00	46.64
Fine aggregate	0-5 mm, Granitic rock, St-Hippolyte quarry (dry)	838.00	46.09
Set retarder	Daratard 17, Grace	872.73 ml	48.00 ml

Specimen fabrication and all exposure regimens were carried out at McGill University laboratory facilities (Montreal, Canada) as described in Hartell' (2014) dissertation. For the purpose of this

study, only the concrete mixture proportions are presented in Table 3.1. Refer to Hartell (2014) for further details on the materials used in the making of the concrete mixtures along with their means of quality control, details on sample fabrication and the curing procedure implemented for these specimens, and their exposure regimes (Figure 3.1).

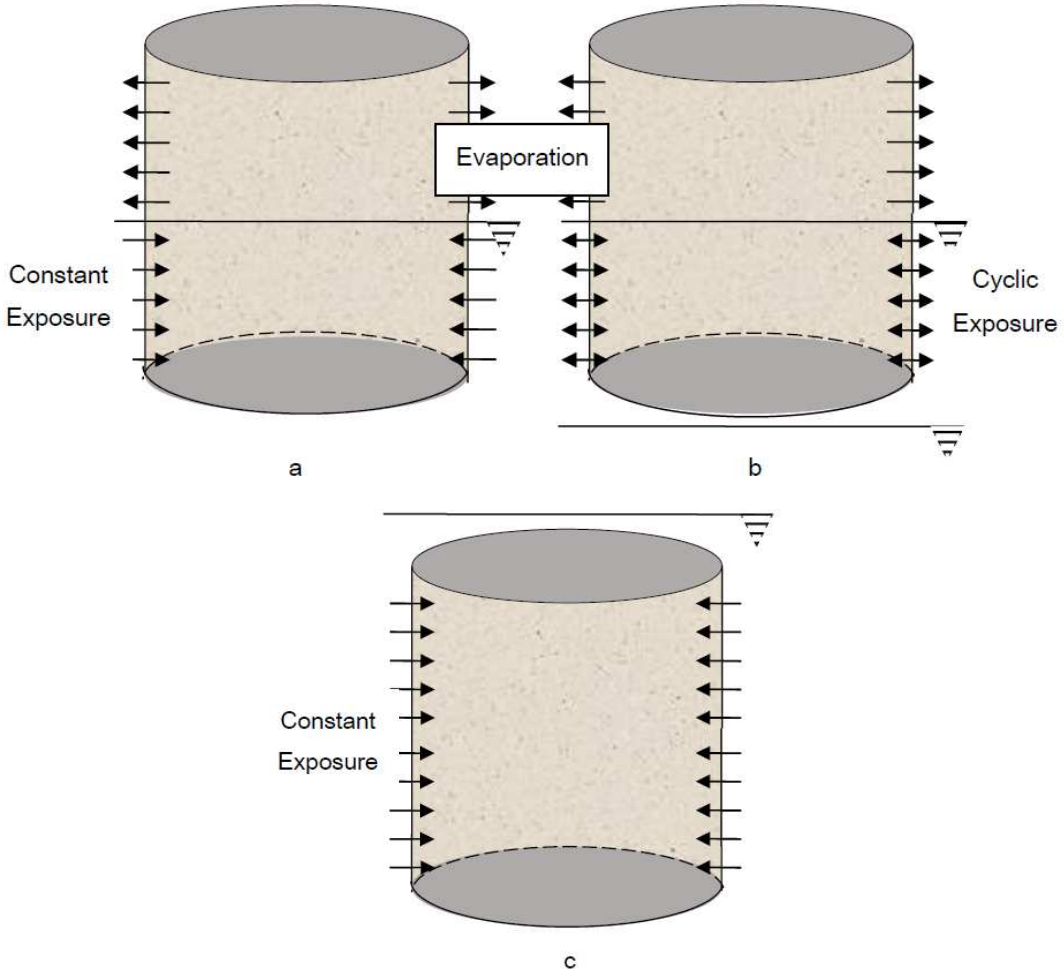

Figure 3.1: Bi-dimensional transport mechanisms for cylinder samples: a) wicking, b) wicking combined with absorption/ evaporation cycles and c) diffusion.

(Hartell 2014)

As discussed in the literature review, different exposure conditions and different means by which the water born sulfate ion may enter mature concrete cause diverse deleterious effects. The

concrete cylinders were exposed to a 5% sodium sulfate solution in three different manners in order to replicate the following solution transport mechanisms:

- diffusion and wicking accomplished by partial immersion of cylinder (Figure 3.1a);
- cyclic sorption/evaporation and wicking accomplished by cyclic partial immersion of cylinder (Figure 3.1b);
- diffusion only accomplished by complete immersion of sample (Figure 3.1c).

The samples were exposed to the solution for a period of two years. Each regimen were carried-out in a connected tank system to ensure that all ponding samples were subjected to the same solution at any given time (Figure 3.2). This eliminated the variation in exposure parameters arising when using multiple separate tanks.

Figure 3.2: Specimens cured in sodium sulfate solutions in controlled conditions.

(Hartell, 2014)

Also, the cyclic exposure was conducted twice per day, this means 6 hours exposed to the solution followed by 6 hours exposed to ambient laboratory conditions. Moreover, both end faces

of the cylinders were sealed with epoxy to create a bi-dimensional transport mechanism where the corner effect was eliminated due to the continuous circular exposure surface of the cylinder. The setup was housed in a temperature controlled closed room with constant exhaust ventilation. The ambient room temperature was kept at 23°C. Temperature readings of the exposure solutions were taken periodically in the tanks. Temperatures recorded ranged between 21.4°C and 23.7°C. (Hartell 2014)

At the end of the 2 year exposure term, the specimens were carefully dry-cut in half along the longitudinal axis and subsequently polished (mirror finish) for microscopy analysis (Figure 3.3). The specimens were labeled according to their exposure regimen and exposure age. Table 3.2 describes the sample nomenclature used for easy reference in the following chapters. Finally, the samples sealed in plastic wrapped and stored in sealed plastic bags to prevent variances in moisture conditions. The samples remained in ambient laboratory temperature conditions until prepared for mXRF analysis.

Table 3.2: Specimen nomenclature used in this thesis

Type of sample	Curing time	Concentration of solution	Transport Mechanism
C: Cylinder	24	LWO: Limewater	A: Diffusion
		SS5: 5% Na_2SO_4	C: Cyclic Sorption/Evaporation
			W: Wicking
			F: Field

Since the cylinder halves were too long to fit on the sample stage, they were further cut into three pieces along the diametric axis as seen in Figure 3.3. In order to minimize loss of sample due to cutting, the middle sections were scanned prior to cutting them; hence, the area scan was done over 90-130mm.

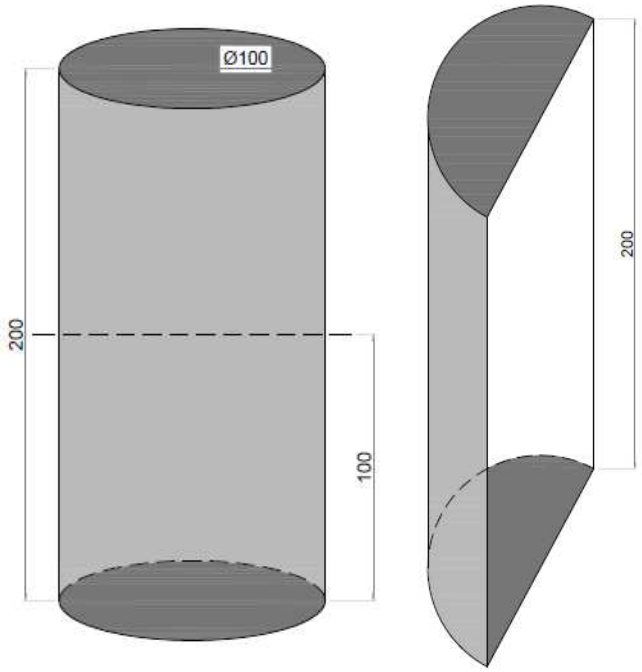

Figure 3.3: Specimen with an immersion line at 100mm and cylinder-half cut along longitudinal axis.

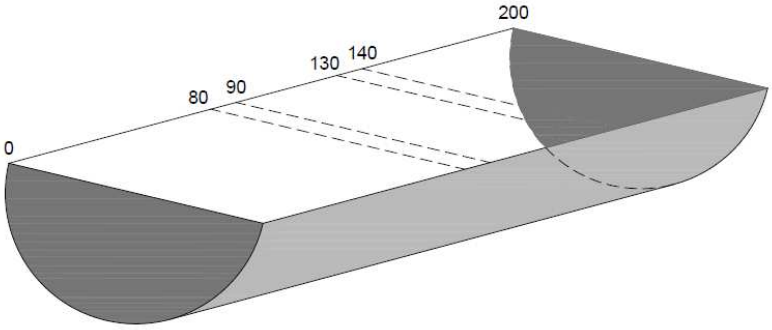

Figure 3.4: Break down into 3 pieces for effective scanning

3.2 mXRF Scanning Procedure

The basic principles of microscopic X-ray fluorescence analysis is illustrated in Figure 3.4. The micro analytical variant of bulk XRF is based on the localized excitation and analysis of a microscopically small area on the surface of a larger sample. The detected signal provide

information on the lateral distribution of major, minor and trace elements in the material under study. Essentially, a beam of primary X-rays with a small cross-section irradiates a sample. The material responds by emitting fluorescent radiation which carries information on the local composition of the sample. Therefore, the radiation is collected using a suitable detector system and subsequently computed. The operator defines the type of scan desired (either spot analyses, line analyses or image collection) along with the location of area to analyze and the computer controlled sample stage automatically moves the specimen in the path of the X-ray beam path. (Peter, 2003)

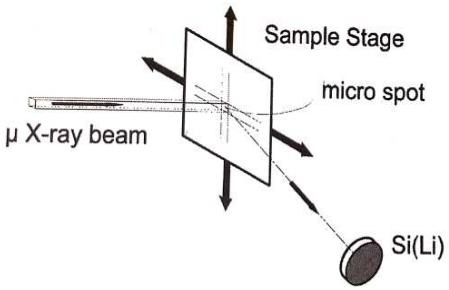

Figure 3.5: Irradiation geometry during μ-Xrf measurements

For this study, low magnification spectral mapping is performed using EDAX software. Al(25μm) shutter filter was used since it reduces the artifact peaks of sulfate detection in concrete.

3.2.1 Middle Section of Concrete Sample

The basic settings include counts per second, dtm values, vacuum pressure, type of filter, peak integral and ROI data.

Table 3.3: Details of apparatus setup and area scan

Name	21W	21A	21 F
Date	3/19/2014	4/4/2014	4/9/2014
Elements	Mg, Al, Si, S, Cl, K, Ca, Ti, Mn, Fe	Mg, Al, Si, S, Cl, K, Ca, Ti, Mn, Fe	Mg, Al, Si, S, Cl, K, Ca, Ti, Mn, Fe
Settings			
Shutter	Open	Open	Open
X-rays	On	On	On
Filter	25 um Al	25 um Al	25 um Al
Vacuum	0.85 TORR	0.85 TORR	0.85 TORR
kV	40	40	40
uA	1000	1000	1000
AmpTime	0.8	0.8	0.8
Z	50	51.69	51.235
Cps	40000	57000	45000
Dtm	10	11	9
Montage			
Filename	lowmag 7X7	lowmag 7X7	lowmag 7X7
Folder	sulfa	21 A	21 A
W	277/41.78/1.64	277/41.78/1.65	266/40.12/1.65
H	358/41.98/1.65	358/41.98/1.66	253/29.67/1.66
Map			
Resolution	0.05	0.05	0.05
X	836	836	802.4
Y	840	840	93.4
Dwell	400	400	400
kV limit	10	10	10
Filename	sulfa	21 A	21 W
Subfolder	TD	21 A	21 W
Folder	Sulfate-Julie	Sulfate-Julie	Sulfate-Julie
Est. Time	24 Hr	24 Hr	24 Hr

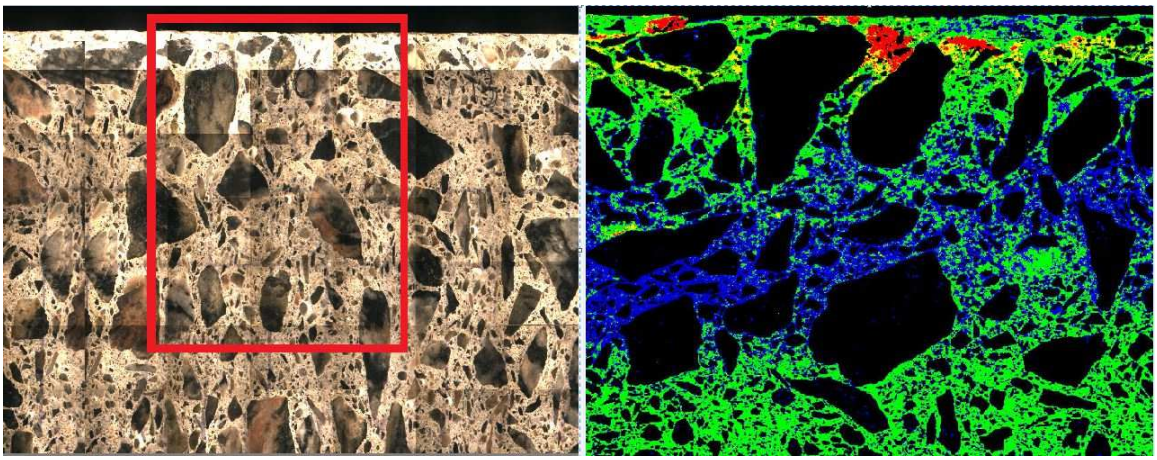

Figure 3.6: 24SS5A sample mapping image in the multi-color sulfur phase map

Figure 3.6 illustrates the area, delineated in red, scanned and the number of counts were recorded for each point measurement. From the latter, it is possible to produce the elemental images of the desired elements. For example, the above image demonstrates a sulfur profile based on the counts intensity (low in blue to high in red).

3.2.2 Bottom Section Of Concrete Sample

Table 3.4: Bottom Section of Concrete Sample

Sample	24SS5A	24SS5W	24SS5F
Matrix	1024	2048	2048
No: of scans	10	20	20
Dwell Time	400µs	400µs	400µs
Time/Scan	8 min/scan	16 min/scan	16 min/scan

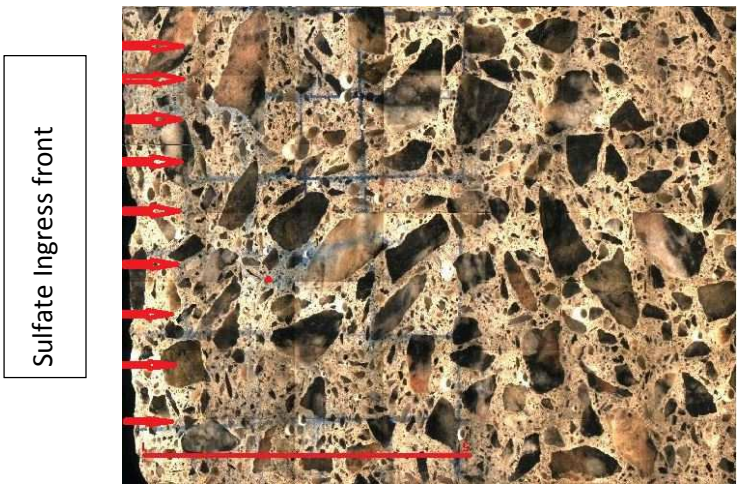

Figure 3.7: Example of line scan image of bottom section

Each bottom section of the samples were placed on the stage and different number of line scans were performed. In this case, since the wicking and field type are in partially saturated conditions, 20 line scans are performed at a span of 3mm for each case to get a clear profile of the sulfate ingress. The number of line scans is decreased for diffusion specimens for making an effective use of the available funds.

This mechanism follows the same principle but instead of area scan, it takes number of point scans on a line making it an effective measure for fast scans with a rough data. Although elemental mapping images are not obtained by line scan, the spectrum energies of different elements at different depths is obtained, making it a quick quantitative tool.

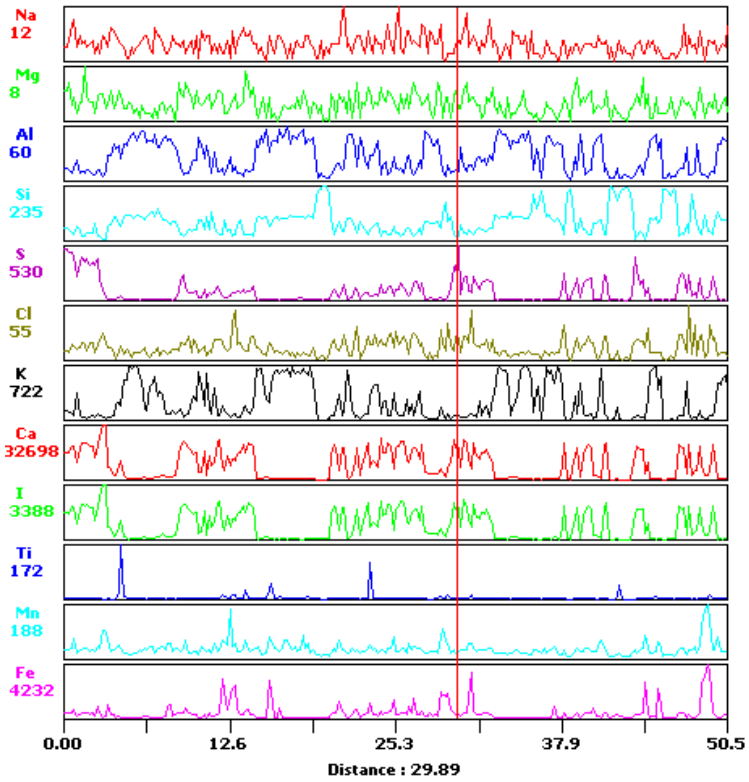

Figure 3.8: Graphs showing distances of concrete specimen verse spectrum numbers.

The peaks are identified by just moving the bar. The concentration and spectrum counts are obtained from the EDAX, to plot the sulfate profile across that line.

Table 3.5: Top Section of Concrete Sample

Sample	24SS5A	24SS5W	24SS5F
Matrix	512	1024	512
No: of scans	10	10	10
Dwell Time	400µs	400µs	400µs
Time/Scan	4 min/scan	8 min/scan	4 min/scan

In this case, the number of line scans is decreased because the major portion near the immersion line is thoroughly scanned with the help of area scan. 40 mm above the immersion line is of less interest when compared to the saturated sections and middle sections showing capillary suction.

Yet, to know the profile of sulfate ions on the top section, minimum number of line scans are performed, by keeping in mind about the cost-effectiveness ratio.

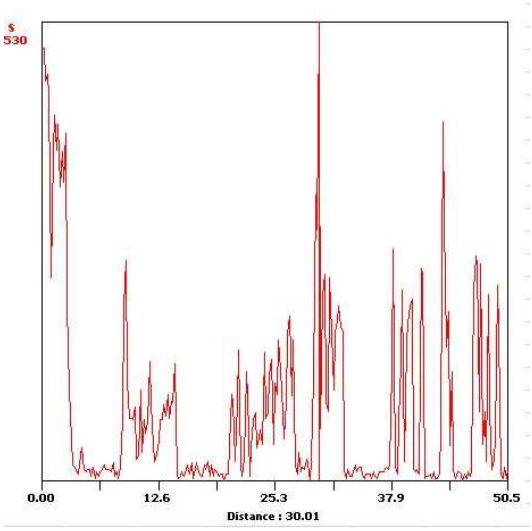

Figure 3.9 Graphical representation of the available sulfate ions on the line.

3.3 Calibration Curve

In order to convert the number of counts obtained from the analysis to actual percent weight concentration values, a calibration curve was prepared using the same cement, admixture and sodium sulfate salt used in the preparation of the specimen. First, paste samples were prepared with the same water-to-cement ratio as the specimen. The paste was then grounded into a fine powder. Thereafter, a known quantity of paste powder was intermix with a known quantity of sodium sulfate salt. Knowing the SO3 content in the cement from the cement mill test report and the elemental composition of Na2SO4, the sulfur concentration of the powder analyzed (figure 3.10) was determined. For each sample prepared, a sulfur concentration was thus associated with the number of counts obtained. The plotted values, Figure 3.11, was then used as a calibration curve to convert counts above background into concentration of sulfur, thus making the result analysis quantitative.

Figure 3.10: Sample preparation for calibration

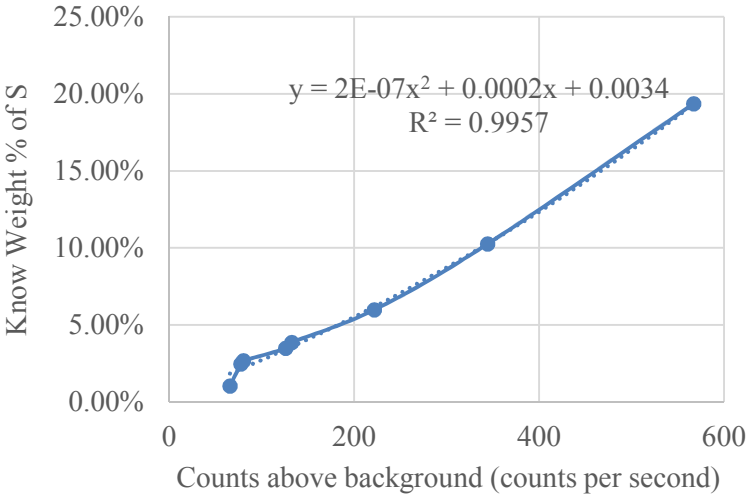

Figure 3.11 calibration curve

3.4 Analysis on Control Samples

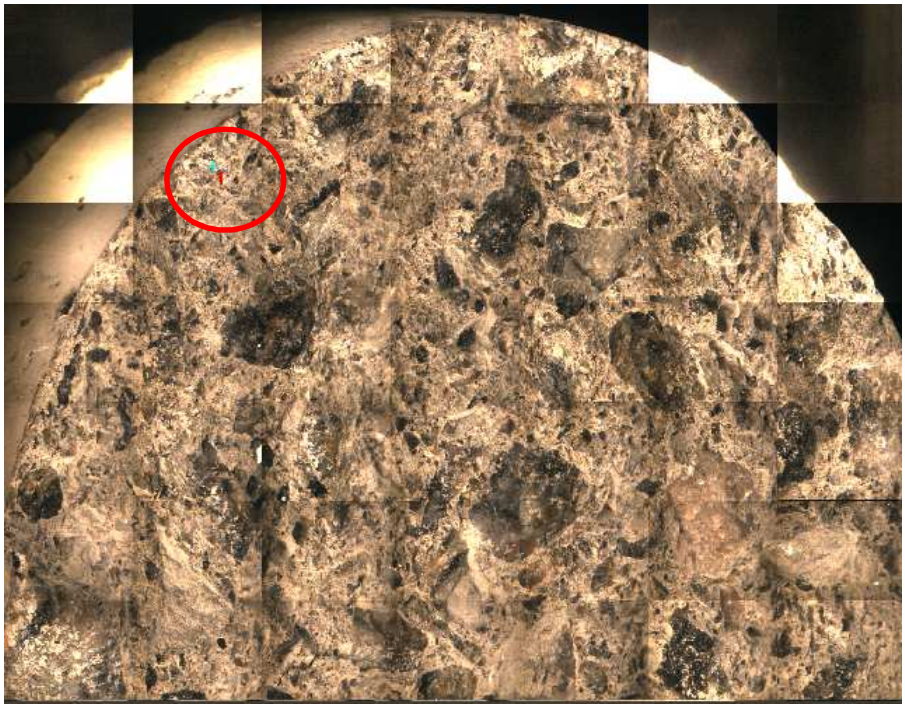

Figure 3.12 Lime water control samples

To validate that the measured amounts of sulfur above baseline for the sulfate degraded concrete samples were indeed from an external source a few point scans were conducted on a control sample. The control specimens were submerged in lime-saturated water to avoid the leaching of alkalis and calcium compounds in cementitious matrix for a period of 24 months (Hartell, 2014).

A control sample was scanned using point scans and compared with the values obtained for the prepared cement paste sample. Figure 3.12 shows one of the point which is scanned to detect the available sulfur in control specimens. Once the counts were converted into concentration values, it was found that the sulfur concentrations measured were indeed similar to the measured counts obtained for the paste samples.

CHAPTER 4

RESULTS AND DISCUSSION

The following contour graphs depict the concentration profile of sulfur element in the concrete blocks. These concrete blocks are partially submerged in 5% sodium sulfate solution for two years. The sulfur quantity in the below graph is termed as milligram of sulfur present in milligram of concrete. The graph is designed in rainbow palate so that the sulfur concentration is quantified from low to high using these seven VIBGYOR colors. X-axis depicts the depth of penetration in concrete block and the Y-axis on the other hand is the width of penetration. The concrete block is cut into three pieces to scan the sample easily through m-XRF machine which is sensitive to large areas.

Using the calibration curve and mill chart reports, the calculated average background sulfur available in the 0.48 w/c ratio concrete mix is 1.03% and this is again crosschecked by scanning the basic limewater samples which were not subjected to any sulfate solution.

In this graph the initial range from 0 to 1.03%, which is shown in black, is termed as baseline sulfur and it is common for all concrete samples tested. The range above 15% is shown in white and is not considered in our ESA analysis.

4.1 Diffusion Transport Regime

As seen in Figures 4.1, the sulfate ingress front extends only for the first few millimeters, up to a maximum of 10 millimeters in depth. The sulfur concentrations level measured surpass 15% which may indicate the presence of a sulfate compound such as gypsum. Further chemical analysis would be required to confirm the product formed.

Pass the ingress front of high concentration towards the bulk (middle) of the concrete samples, there are areas above the sulfate baseline concentration but these remain low, below 3% sulfur concentration. In a few instances, concentration peaks, around 7%, are measured within these areas. This is well depicted in the area scan for the middle section of the sample. This is noticed throughout the sample height. Here, the diffusion process may have contributed to the migration of ions within the porous structure. This process is known to be slow explaining the presence of "Sulfur Island" as opposed to a uniform and widespread ingress. Moreover, as described by Santhanam et al. (2002) the newly formed products of sulfate attack will generate microcracks within neighboring material. These will facilitate ionic transport pass the initial ingress front to further react with the paste within. This process is well depicted in Figure 4.1 presented in the literature review and corroborates with that seen on the sulfur map.

However, external sulfate attack encountered in the field are rarely driven by diffusion only; therefore, evaluating sulfate ingress in the presence of an evaporation front and cyclic evaporation and sorption is of importance.

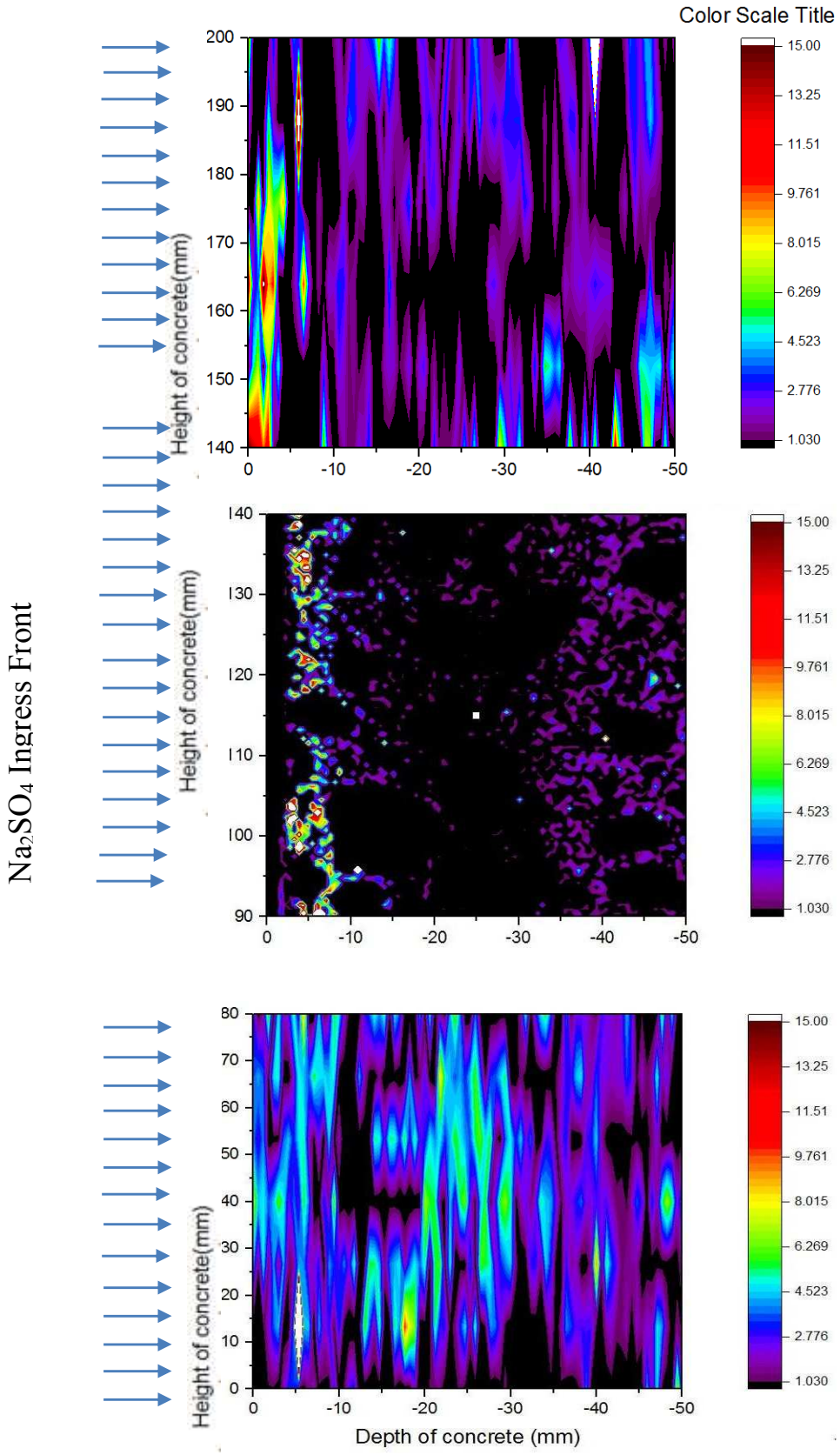

Figure 4.1 Contour map showing the profile of sulfate ions for specimen 24SS5A.

4.2 Wicking transport regimen

When dry surface of concrete is exposed to sulfate solution, the porous concrete structure acts like a sponge by absorbing the ion solution through capillary action. In this case only half of the sample is saturated with sodium sulfate solution, leaving the rest exposed to the ambient conditions. With the presence of an evaporation front, the above dry surface furthers capillary action creating a wicking transport mechanism. The wicking mechanism is seen due to the vapor conduction from wet surface to the dry surface. Due to the diffusion of vapor ions, the deposits of salt crystals are left out in the pore structure (Thomas et al., 1995). This process is also known as salt weathering. The physico-chemical reactions of formation of ettringite and gypsum and then followed by scaling due to the formation of crystal growth in the pores. This phenomenon leads to surface deterioration and efflorescence (Zanqun Liu et al.). Looking at the upper half of the sulfur map, the latter is observed as high concentration levels are found passed the immersion line, over the entire depth of the concrete specimen. Here sulfates seem to have traveled as high as 200mm (over the entire height) following the evaporation path towards the outer surface of the samples. The larger concentrations found near this surface would correspond to the recrystallized sulfate salts which led to visual signs of surface scaling.

According to Boyd and Mindness, 2004, the presence of such a wicking mechanism would draw larger amounts of sulfate through the matrix as opposed to a diffusion mechanism alone. Comparing Figure 4.1 with the bottom portion of the sulfur map of Figure 4.2, it is clear that the wicking mechanism as increased the penetration front passed 10mm. Moreover, as depicted previously, the presence of sulfur islands are found across the bottom half of the cylinders, reaching concentrations above 8%. This is larger than that found for the diffusion mechanism.

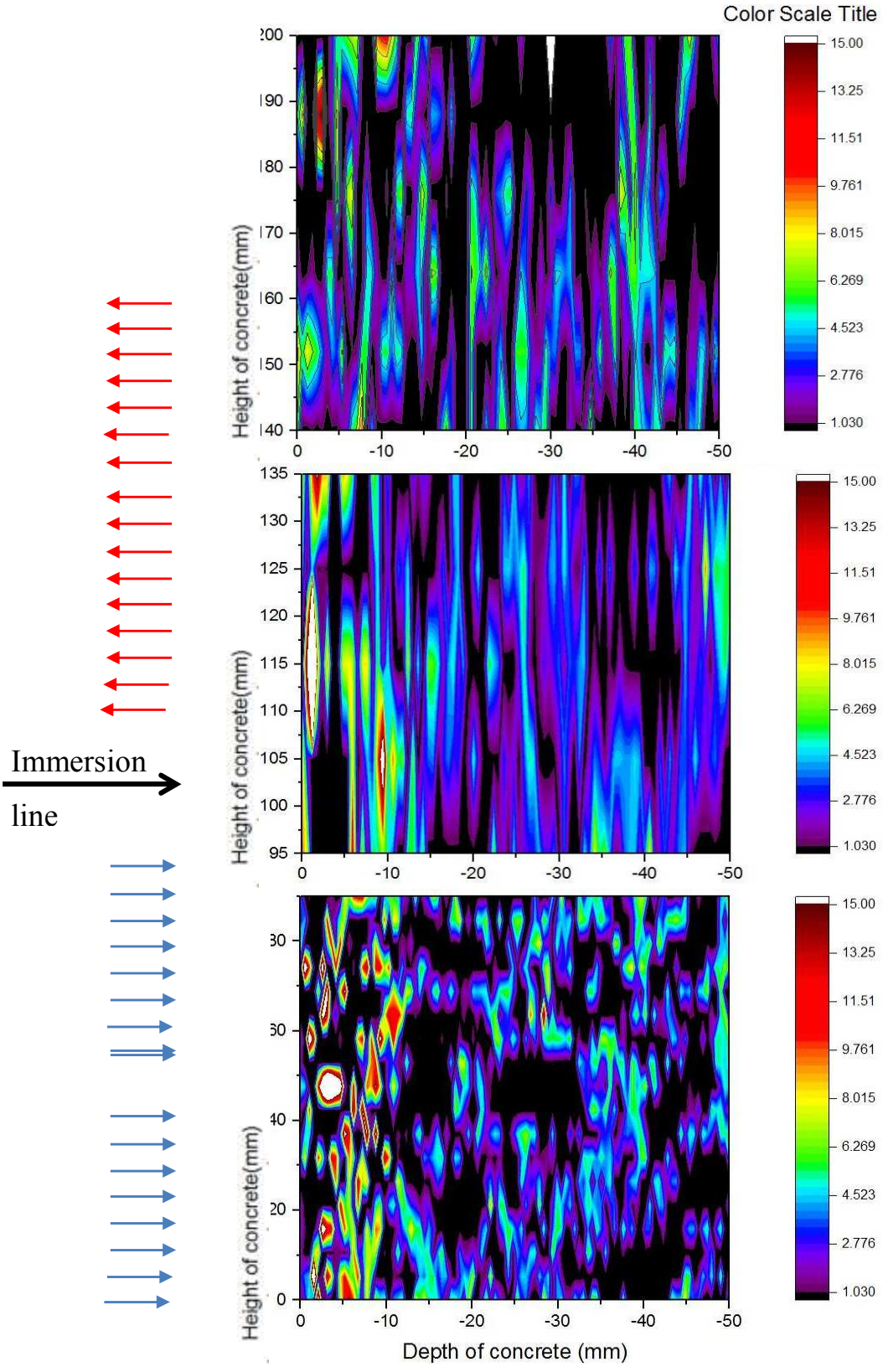

Figure 4.3 Contour map showing the profile of sulfate ions for specimen 24SS5W.

4.3 Field Transport Regimen

The field transport mechanism was achieved by cyclically immersing the bottom half of the concrete cylinder in the sulfate laden solution and exposing the upper half to ambient room temperatures and moisture conditions. Hong 1998 stated that by cycling the solution exposure, creating wet-dry cycles, sulfate uptake would be accelerated via capillary sorption. According to Moukwa, 1990, the sulfates would ingress deeper into the concrete as the number of wet-dry cycles increases. In comparison to the sulfur profile obtained for the previous diffusion specimen, there is no clear evidence of this fact. The ingress front for the bottom half, subjected to wet-dry cycles, is at approximately 5mm. And, as see for the diffusion mechanism, there are islands of low sulfur concentration across the cylinder core. Here, the samples will be further investigated to validate these findings.

Looking at the upper half of the sulfur map (above the immersion line at 100mm), high concentrations of sulfur are found only near the surface of the specimen, between 0 and 10 mm Opposite to that seen in Figure 4.2, here the presence of an evaporation front creating a wicking transport mechanism did not seem to draw more sulfates within the bulk of the microstructure. And, only a low concentration of sulfates is found above the immersion line..

However, physical damage induced by recrystallization pressure was visually noticed on the samples. The wicking phenomena may be responsible for the surface damage noticed but at a lesser extent than that noticed for the previous sample. Scaling damage was noticed between 110 mm and 140 mm which correspond to the area where high sulfur concentrations are present (above 15%) on Figure 4.3.

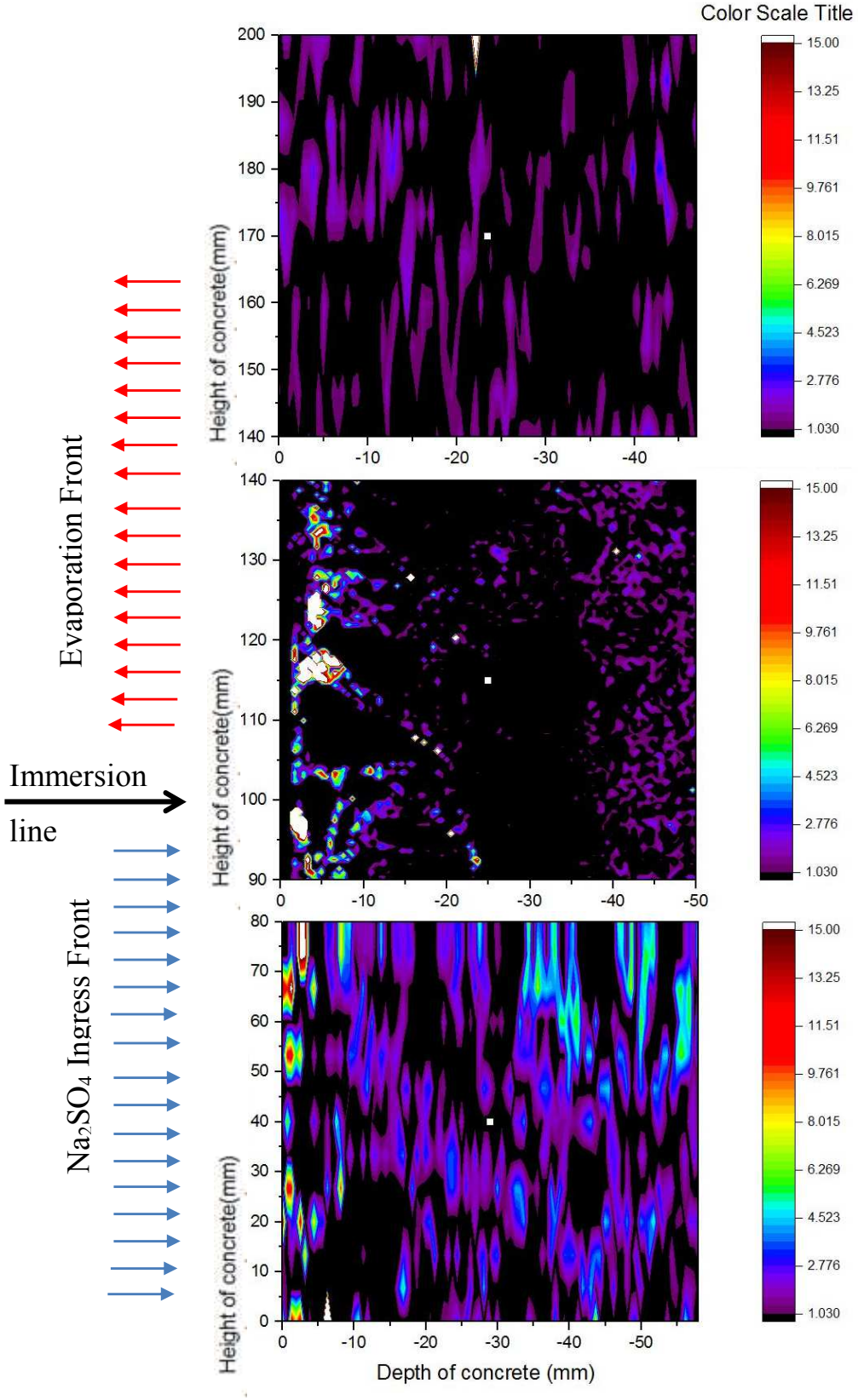

Figure 4.3: Contour map showing the profile of sulfate ions for specimen 24SS5F.

CHAPTER 5

CONCLUSION

The use of milli-X-ray fluorescence -X-ray spectrum imaging is found to be a good analysis tool to perform the chemical profiling of sulfate ions into the concrete. From this research, the technique used provided a general understanding of the different transport mechanisms involved for the three exposure regimens replicated in the laboratory. The two-dimensional sulfur concentration maps created were consistent with past investigations on sulfate attack using other forms of investigative techniques.

As expected, the ingress front for the diffusion transport mechanism (completely immersed specimen) was the lowest, below 10 mm; accompanied by a low bulk concentration of sulfur. For the partially immersed samples, the presence of an evaporation front and a moisture gradient within the sample did contribute to drawing a larger quantity of sulfates with the porous material. For the submerged half, the high concentration ingress front surpassed 10mm and areas in the bulk material reached concentrations above 8%. Moreover, it would seem that sulfates traveled within the bulk material through capillary action up the entire height of the cylinder, leaving high concentrations of sulfur near the evaporation plane at the surface of cylinder. As for the field transport mechanism, similar results were expected for the partially immersed sample subjected to wet-dry cycles. Instead, the cyclic exposure did not contribute to extending the ingress front, sulfate penetration was found to be less than that observed for the diffusion regimen. The presence of an evaporation plane did contribute to the settlement of sulfate compounds near the

surface of the material, directly above the immersion line; although, the bulk concentration remained low (below 3%).

To better understand the results obtained and associate them with the formation of know products of sulfate attack: gypsum, ettringite and various salts, it is recommended to combine the method with other analytical means such as X-ray diffraction and scanning electron microscopy with energy dispersive spectroscopy. Moreover, the area scan provided a better visual interpretation of the concrete's physical microstructure because of the differences between elemental composition between aggregate and paste and because of the porous nature of the material providing space for crystal formation. Still, the contour plots created from the line scan measurements were sufficient to obtain concluding results.

REFERENCES

"External Sulfate Attack." Www.concrete-experts.com. N.p., n.d. Web.

"Lucideon." XRD Analysis. N.p., n.d. Web. 09 July 2015.

A, Bonakdar, and Mobasher B. "Multi-parameter Study of External Sulfate Attack in Blended Cement Materials." Construction and Building Materials 24.1 (2010): 61-70.

Basheer L. Assessment of the durability characteristics of surface treated concrete, PhD Thesis. The Queen's University of Belfast, 1994:296.

Bonen D, Cohen MD. Magnesium sulfate attack on portland cement paste - I. Microstructural analysis. Cement and Concrete Research. 1992;22(1):169-80.

Boyd, A.J. and Mindess, S.: :The Use of Tension Testing to Investigate the Effect of W/C Ratio and Cement Type on the Resistance of Concrete to Sulfate Attack". In: Cement and Concrete Research 34 (2004), pp. 373-377

Brouwer, Peter. Theory of XRF. PANalytical, 2003.

Gollop RS, Taylor HFW. Microstructural and microanalytical studies of sulfate attack III. Sulfate-resisting portland cement: Reactions with sodium and magnesium sulfate solutions. Cement and Concrete Research. 1995;25(7):1581-90.

Gollop RS, Taylor HFW. Microstructural and microanalytical studies of sulfate attack. I. Ordinary portland cement paste. Cement and Concrete Research. 1992;22(6):1027-38.

Hartell, Julie Ann. “Investigating various test methods for assessing the effect of sulphate attack on concrete properties”. Thesis. McGill University, 2014

Hong, Katherin. "Cyclic Wetting and Drying and Its Effects on Chloride Ingress in Concrete." University of Toronto (1998): n. pag. Web.

Irassar, Edgardo F. "Sulphate Attack and Sulphate Resistant Cements." Advances in Cement Technology (n.d.): 595. Web.

Jakobsen, Ulla Hjorth, and Claus Pade. "External Sulfate Attack." Concrete Experts International.

Kurtis, K.E., P.J.M. Monteiro and S.M. Madanat (2000) “Empirical Models to Predict Concrete Expansion Caused by SulphateAttack,” ACI Materials Journal,March-April, 156-161

Lorente, Sylvie, Marie Pierre Yssorche -Cubaynes, and Jérome Auger. "Sulfate Transfer through Concrete: Migration and Diffusion Results."Cement and Concrete Composites 33.11 (2011): 735-41. Web.

Lulu, Basheer, and Joerg Kropp. "Assessment of the Durability of Concrete from Its Permeation Properties: A Review." Construction and Building Materials 15.2-3 (2001): 93-103.

Marchand, J., E. Samson, Y. . Maltais, and R. J. Lee. "Predicting the performance of concrete structures exposed to chemically aggressive environments - field validation." (2002): n. pag.. 5 June 2002.

Matschei T, Lothenbach B, Glasser FP. “The AFm phase in Portland cement”. Cement and Concrete Research. 2007;37(2):118-30

Micro X-ray Fluorescence (μXRF). XOS, n.d..

Moukawa, M., 'Deterioration of Concrete in Cold Sea Waters', Cernent and Concrete Research, v20, n3, May 1990, p439 – 44

Permeability testing of site concrete — a review of methods and experience, Report No. 31The Concrete Society (1987)

Peukert S, Garbacik A, Chladzynski S. Cement sulfate resistance evaluation by the draft European standard of direct testing method. In: Dhir RK, Dyer TD, eds. Modern concrete materials: binders, additions and admixtures 1999.

Santhanam M, Cohen MD, Olek J. “ Effects of gypsum formation on the performance of cement mortars during external sulfate attack. Cement and Concrete Research”. 2003;33(3):325-32

Santhanam, M., Cohen, M. D. and Olek, J.:” Sulfate Attack Research – Whither Now?”. In: Cement and Concrete Research 31(2001), pp.845-851

Santhanam, Manu, Menashi D. Cohen, and Jan Olek. “Mechanism of Sulfate Attack: A Fresh Look Part 2. Proposed Mechanisms” Digital image. Cement and Concrete Research 33 (2003) 341–346. N.p., 31 July 2002. Web.

Stroh, J., M. C. Schlegel, E. F. Irassar, B. Meng, and F. Emerling. "Applying High Resolution SyXRD Analysis on Sulfate Attacked Concrete Field Samples." Cement and Concrete Research 66 (2014): 19-26

Stutzman, Paul E. "Scanning Electron Microscopy in Concrete Petrography." National Institute of Standards and Technology (2001): 59-72.

Sun, Chao, Jiankang Chen, Jue Zhu, , Minghua Zhang, and , Jian , Jian. "A New Diffusion Model of Sulfate Ions in Concrete." Construction and Building Materials 39 (2013): 39-45. Web.

Taylor HFW. In: Telford T, ed. Cement chemistry: Academic Press 1997:118-9 and 26-28.

Tixier, R. and B. Mobasher (2003).“Modeling of damage in cement-based materials subjected to external sulphateattack –part 1: formulation.ASCE Journalof MaterialEngineering, 15, 4, 305–13.

Torres-Luque, M., E. Bastidas-Arteaga, F. Schoefs, and M. Sánchez-Silva. "Non-destructive Methods for Measuring Chloride Ingress into Concrete: State-of-the-art and Future Challenges." Construction and Building Materials 68 (n.d.): 68-81.

Weritz F, Ryahi S, Schaurich D, Ta□e A, Wilsch G. “Quantitative determination of sulfur content in concrete with laser-induced breakdown spectroscopy”. Spectrochim Acta B 2005; 60:1121–31.

Liu, Zanqun, Dehua Deng, and Zhiwu Yu. "“Salt Weathering” Distress on Concrete by Sulfates?" Magnel Laboratory for Concrete Research, Department of Structural Engineering, (n.d.): n. pag.

A, Thomas M.D, and Martin Perez. "Service Life Modelling of Reinforced Concrete Structures Exposed to Chlorides." A Literature Review,. Department of Civil Engineering (n.d.): n. pag. University of Toronto. Web.

SUDBRINK, BRYAN. "INVESTIGATION OF SILANE TREATMENTS IN CONCRETE USING VARIOUS NON-DESTRUCTIVE TECHNIQUES." Thesis. OKLAHOMA STATE UNIVERSITY, 2013.

VITA

HARISHMA DONTHINENI

Candidate for the Degree of

Master of Science

Thesis: CHEMICAL PROFILING OF SULFATE DETERIORATED SAMPLES USING MILLI X-RAY FLUORESCENCE -X-RAY SPECTRUM IMAGING

Major Field: Civil Engineering

Biographical: Harishma Donthineni was born in Visakhapatnam, Andhra Pradesh, India on July 19th, 1991. Her parents are Nageswara Rao Donthineni and Bhagyalakshmi Donthineni.

Education:

Completed the requirements for the Master of Science in Civil Engineering at Oklahoma State University, Stillwater, Oklahoma in July, 2015.

Completed the requirements for the Bachelor of Science/Arts in Civil Engineering at Gayatri Vidya Parishad College Of Engineering, Visakhapatnam, Andhra Pradesh, India in 2013.

Experience:

Graduate research assistant at Oklahoma State University, Stillwater, Oklahoma, August 2013-Decemeber 2013.

Graduate Teaching Assistant at Okalhoma State University, Stillwater, Oklahoma, January 2014-Decemeber 2014.